Mechanistic Insight into Porous Electrode Impedance: An Example of Ni+YSZ Cermet Anodes

A. Nenning[a,b], M. Gerstl[a,b], M. Bram[a,c] and A.K. Opitz[a,b]

[a] Christian Doppler Laboratory for Interfaces in Metal-Supported Electrochemical Energy Converters, Vienna, 1060, Austria
[b] Vienna University of Technology, Institute of Chemical Technologies and Analytics, Vienna, 1060, Austria
[c] Forschungszentrum Jülich GmbH - IEK-1, Jülich, 52425, Germany

Optimization of SOFC electrodes requires detailed insight into their electrochemical processes and rate limiting steps. The impedance spectroscopic investigation of symmetrical cells with two equal electrodes on a solid electrolyte measures not only the area-specific polarization resistance of the electrodes, but physically motivated equivalent circuit modelling and fitting also gives detailed insight into the electrochemical reaction mechanisms and rate limiting processes. In this paper, we give a comprehensive introduction into impedance modeling of porous electrodes and show that a transmission-line type equivalent circuit that is mathematically analogous to the Adler-Lane-Steele model is perfectly applicable to Ni+YSZ cermet anodes. The equivalent circuit fit yields the effective ionic conductivity of the cermet structure, which enables determination of the YSZ phase tortuosity factor. In addition, we can measure the characteristic electrochemically active thickness of the anodes, which gives a direct guideline for the optimal thickness of the fine grained anode active layer in a full SOFC.

Introduction

New materials and processing techniques for SOFC electrodes have the potential to drastically decrease the polarization resistance, and thereby lower the operation temperature and increase the power output and efficiency of SOFC systems. However, targeted optimization of electrodes requires good mechanistic insight into the kinetics of electrochemical reactions and ion conduction. Due to the many processes that happen during a DC or impedance spectroscopic test of a full cell, mechanistic information on individual electrode processes is hard to get. Impedance measurements on symmetrical electrolyte supported cells with two equal oxygen or fuel electrodes yields much better insight, while maintaining electrode processing steps equal to the full cell. Even without equivalent circuit modelling, the area specific resistance of one electrode can be measured. With proper impedance modelling and equivalent circuit fitting, even detailed mechanistic insight can be gained.

In general, not only the electrochemical oygen reduction, or fuel oxidation reaction, but also ion and electron conduction often significantly influence the impedance and total polarization resistance. However, their interplay is rather complex and can usually not be described either by simple parallel or serial connections of discrete resistors. This complex

mathematical description of the conduction, diffusion and reaction processes and their relation to the AC impedance was already derived in 1997 by S.B. Adler et al (Adler-Lane-Steele or ALS model) (1), and exemplified on SOFC cathodes (2–4). Mathematically isomorphic impedance models were around the same time also derived for different electrochemical systems such as porous electrodes immersed in a liquid electrolyte e.g. by Bisquiert et al (5,6). The latter is also available in the widely used equivalent circuit fitting software Zview, and it was proven to be appropriate to describe the impedance of LSM-YSZ composite cathodes. (7)

All of these models are based on the concept of an isotropic porous electrode structure, in which the geometric features (particles, pores, sinter necks) are very small compared to the total thickness of the electrode (7). Therefore the electrode can be treated as an effective single phase homogeneous medium, with average values for surface area density, triple phase boundary density, porosity and effective ion/electron conductivity. This simplification tremendously simplifies the mathematical description of electrochemical properties to an effectively one-dimensional model. The electrical properties of such an electrode can then be either described by differential equations and their mathematical solution, as in the ALS model, but also a graphical representation in form of an equivalent circuit is possible, and for the sake of comprehensiveness we will focus on the latter approach here. Interestingly, the impedance of almost any porous electrode, in which electronic and ionic charge carriers are present can be described by mathematically very similar models, which can be represented by a transmission-line type equivalent circuit.

Transmission-line Type Equivalent Circuits for Porous Ni+YSZ Cermet Electrodes

This section just gives a short introduction into the impedance modeling of porous electrodes, and focuses on the example of Ni+YSZ cermets. For more details in impedance modeling, we suggest publications focusing on impedance modeling (8) and simulation (9) for SOFC anodes, or SOFC cathodes (1,3,7). When the average particle size is below approximately 1 μm, meaning that the structure can be approximated by a homogeneous medium, the electrical potentials of electron and ion conducting phase mainly depend on the distance from the electrolyte (z). In this condition, a quasi one dimensional impedance model, depending on the distance from the electrolyte-electrode interface is sufficient to describe the impedance of such an electrode. The mathematical motivation is as follows: The electrochemical hydrogen oxidation reaction takes place at the triple phase boundary, where gas phase, Ni and YSZ meet. Therefore it can be written as

$$H_{2,gas} + O^{2-}_{YSZ} \rightleftharpoons H_2O_{gas} + 2e^-_{Ni}. \qquad [1]$$

Without applied voltage, this reaction is in equilibrium. For now we assume fast gas phase diffusion, meaning that partial pressures and chemical potentials of H2 and H2O are independent of the cell current. In equilibrium, the electrical potentials in the YSZ and Ni phase are usually not identical, due to the electrochemical double layer forming at the interface. A voltage is applied to the electrode will change the electrical potentials of Ni and YSZ phase relative to their equilibrium values and drive a net reaction rate. This also causes shift of the electrochemical potentials of electrons in Ni and oxygen anions in the YSZ, which is entirely caused by the applied voltage. This voltage change is then the

driving force for a net reaction rate of reaction [1]. We can define a local over potential, depending on the distance from the electrolyte (z) as

$$\eta(z) = -\frac{\Delta_R G}{2F} = \frac{\Delta\tilde{\mu}_{ion,YSZ} - 2\Delta\tilde{\mu}_{eon,Ni}}{2F} = \Delta\phi_{Ni} - \Delta\phi_{YSZ}\,, \qquad [2]$$

where $\Delta_R G$ is the Gibbs free energy of reaction [1], and $\Delta\tilde{\mu}_x$ are the changes of electrochemical potentials relative to equilibrium $\Delta\phi_x$ stands for the electrical potential perturbation relative to its equilibrium value. Both the electrical charge stored in the double layer capacitance between YSZ and Ni phase as well as the driving force and net rate of the TBP reaction are proportional to this local overpotential, as long as the overpotential remains small. Mathematically, we can therefore describe the interface capacitance and TPB reaction between Ni and YSZ by a parallel circuit of a non-ideal capacitor C_{dl} (constant phase element) and resistor R_{TPB}.

In addition to the surface reaction, the electrode model must also consider electron and ion conduction along the z-direction, and its associated overpotential losses. This interplay of electrochemical reactions and overpotential losses from ion/electron conduction can be represented in a transmission-line type equivalent circuit, consisting of an infinite number of differential elements. These differential elements are aligned along an electronic and ionic "rail" describing the conduction of electronic and ionic charge carriers, respectively. These rails are coupled by vertical circuit elements, that describe the coupling of electronic and ionic carriers through electrochemical processes, as sketched in Figure 1.

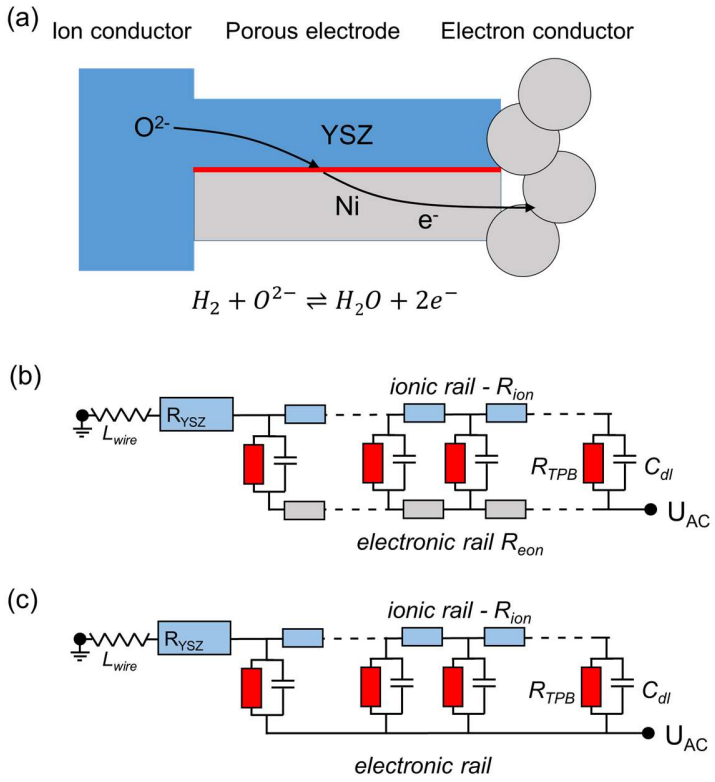

Figure 1. (a) Simplified sketch of ion and electron conduction in a porous SOFC electrode. (b-c) Equivalent circuit models for fitting the impedance spectra, either considering an electrode with moderate (b) or high effective electronic conductivity (c).

The mathematical impedance function of such a transmission line in the most general form was found by Bisquert (6). It should be noted that mathematical symbols differ from the original publication, in order to more intuitively describe their physical meaning in the case of Ni-YSZ cermets, which is given by the equation

$$Z = \frac{R_{ion}R_{eon}}{R_{ion}+R_{eon}}\left(\mathrm{L} + \frac{2\lambda}{\sinh\left(\frac{\mathrm{L}}{\lambda}\right)}\right) + \lambda\frac{(R_{ion}^2+R_{eon}^2)}{R_{ion}+R_{eon}}\coth\left(\frac{L}{\lambda}\right), \quad [3]$$

where

$$\lambda = \sqrt{\frac{1}{\left(\frac{1}{R_{TPB}}+(i\omega)^p \mathrm{Q_{dl}}\right)(R_{ion}+R_{eon})}}. \quad [4]$$

In this model, Z is the area specific impedance with the unit of Ωcm^2, R_{ion} and R_{eon} are the inverse effective ionic and electronic conductivities, R_{TPB} is the effective resistance of the TPB reaction, and L is the thickness of the active electrode layer. The capacitance of the electrochemical double layer forming between YSZ and Ni phase is modeled with a constant phase element (CPE) (10), rather than a capacitor in order to better describe the shape of the spectra. Although there is no straightforward justification for using a CPE instead of a capacitor, non-ideal behavior of double layer capacitances is observed throughout literature, also for thin film model electrodes (11–14).

Effective conductivities of a porous structure are related to the electrode microstructure by the relation (15–17)

$$\sigma_{eff,x} = \frac{1}{R_x} = \frac{\sigma_{bulk}\tau_x}{\epsilon_x}, \quad [5]$$

where x stands for either electrons or ions, σ_{bulk} is the bulk conductivity, ε is the volume fraction of electron or ion conducting phase, and τ the tortuosity.

The rather bulky impedance function from Eq. 1 can be strongly simplified, when the effective electronic conductivity is relatively high, and therefore R_{eon} can be approximated to be almost zero. In literature, an electron conductivity of at least 100 S/cm is often states to be the minimum. However, if a porous current collecting layer is perepared on top of a thin (10-50 µm) anode active layer, an effective electron conductivity as low as 1 S/cm is already sufficient for almost negligible electron conduction resistance in across-plane direction. This simplification reduces equation [3] to

$$Z = \lambda R_{ion}\coth\left(\frac{L}{\lambda}\right). \quad [6]$$

This is now the impedance function associated to the circuit in Figure 1c. For technologically used electrodes, a further simplification is often possible when we assume that the electrode is much thicker than the electrochemically active thickness λ. In this case, the simplification coth(x>>1) ≈ 1 leads to the impedance function

$$Z = \lambda R_{ion} = \sqrt{\frac{R_{ion}}{\frac{1}{R_{TPB}} + (i\omega)^p Q_{dl}}} \quad [7]$$

This impedance function is now equivalent to the Gerischer impedance (18,19) which means that the function is overparametrized and therefore one elementary parameter (Rion, R_{TPB} or C_{dl} must be known and fixed during fitting for a unique fitting result. An example for this will be given in the experimental results section.

Equation [6] is mathematically isomorphic to the Adler-Lane-Steele (ALS) model[1,3,4], The apparent difference to the ALS model is merely because the ALS model is expressed in terms of diffusivities, defect concentraitions and equilibrium reaction rates rather than electrical quantities. In literature, the ALS model was so far only discussed for mixed conducting SOFC cathodes, although we can show that it is also applicable to Cermet anodes, in which oxygen and electron conduction are shared between two different phases. In the experminetal results and discussion section, we will show that the circuit model of Figure 1c, described by the impedance function of equation [6] is perfectly suited for describing the shape of the impedance spectra of symmetrical cells with two Ni+YSZ anodes. Also, the fitted conductivities and kinetic parameters are in line with the bulk properties and model studies that investigate the electrochemical response of Ni pattern electrodes.

Expermiental Methods

Cell Fabrication

Symmetrical Ni+YSZ anode cells were prepared by screen printing of commercial paste by Heareus (CL82-8520A), consisting of 60% wt. NiO and 40% 8 mol% Y_2O_3 doped ZrO_2 (8YSZ). Polycrystalline 8YSZ substrates of 15mm diameter and 0.25 mm thickness purchased from by Kerafol were used. Circular electrodes with 10 mm diameter were printed, dried and sintered at 1350°C for 3 hours. The thickness of the electrodes was varied by using different meshes for screen printing, and afterwards determined by scratching and thickness measurement in a confocal microscope.

Impedance Spectroscopic Testing

Impedance tests were carried out in a single chamber impedance measurement setup. The chamber and cell holders consist entirely of fused silica, Pt wires and Ni foam for electrode contacting, as sketched and depicted in Figure 2. The cells were homogeneously heated in a foldable tube furnace (Carbolite-Gero, Germany) and impedance spectra were measured in 4-wire mode with a PSM 1753 with IAI interface, Newton's Fourth Ltd., UK in a frequency range of 100000-0.1 Hz at 20mV (RMS) AC amplitude in a temperature range of 500-790°C. In order to minimise the gas phase diffusion impedance, several optimisations were made in the testing setup: Firstly, the gap between the electrode contacting Pt sheet and electrode was filled by a highly porous Ni foam (95% porosity, 1.5-2 mm thickness). This soft foam additionally ensures very good electrical contacting, in order to avoid any possible electronic sheet resistance effect. The feed gas line was kept at room temperature, which limits the humidification level to 25-30 mbar. In order to increase the diffusion coefficient of H_2 and H_2O molecules, typical electrochemical tests were

carried out at a reduced pressure of 70 mbar (30 mbar H_2O and 40 mbar H_2). The chamber pressure was regulated by continuous pumping of the chamber, while maintaining a gas feed of about 30 sccm. Before the impedance testing, a blank heating cycle to 1000°C for 12 hours was performed, in order to evaporate possible contaminant species.

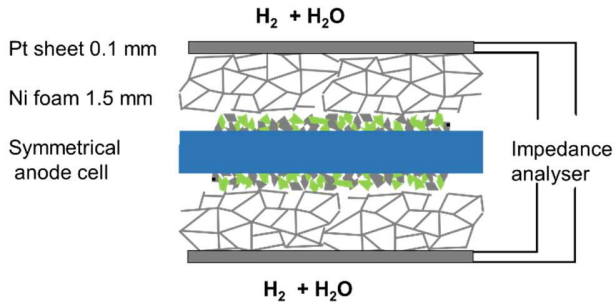

Figure 2. Sketch of mounting and electrical contacting of the symmetrical anode cell.

Impedance Fitting

The measured impedance spectra were first normalised to the electrode area, and fitted, using the commercial software Zview and and the equivalent circuit printed in Figure 1c. The transmission-line impedance is available in Zview, as a distributed equivalent circuit element, called *"DX11-Bisquert 2"*, in which parameter names are rather unintuitive, and their relation to the impedance function in equation [3] is given in the following Table 1.

TABLE I. Relation of Zview fitting parameters to Eq. 3.

Parameter Name in Zview	Parameter name in Eq. 3	Fixed/Free parameter	Unit
DX1	None	11 (fixed)	Not a mathematical expression
DX-R	R_{con}	0 (fixed)	Ωcm
DX-T		0 (fixed)	F/cm
DX-P		1 (fixed)	1
DX-U	R_{ion}	free	Ωcm
DX-A		0 (fixed)	F/cm
DX-B		1 (fixed)	1
DX-C	R_{TPB}	free	Ωcm^3
DX-D	C_{dl}	free	F/cm^3
DX-E	p_{dl}	free	1
DX-F	L	fixed (thickness measurement)	cm

Experimental Results and Discussion

Impedance Spectra Measured in Different Atmospheres

The polarization resistance of the electrodes was measured for two different thicknesses – 14 and 40 µm, in different atmospheric conditions. Visible in Figure 3, the polarization resistance of the electrodes at 790°C strongly depends on the thickness and atmospheric conditions. The effect of three different testing atmospheres is especially pronounced for the 40 µm thick electrodes, which exhibit lower electrochemical polarization resistance. A

pronounced low-frequency feature at 1.5 Hz appears when the cells are tested in humidified forming gas at 1 bar with only 2.5% H_2 and 2.5% H_2O in Ar balance. In line with other studies, we can identify this feature as a rather large gas diffusion impedance in the stagnant atmospheric layer within the Ni contacting foam.(20,21) For Ni+YSZ anodes, the gas diffusion feature is well separated, because the peak frequency of the electrochemical electrode dispersion feature is about 1500 times higher than the gas diffusion peak frequency, as indicated in Figure 3.

The impedance spectra collected at similar H_2 and H_2O pressures, but without Ar balance exhibit no pronounced gas diffusion feature, which proves that the faster gas phase diffusion coefficient can be strongly enhanced when cell tests are carried out at low total pressure (8).

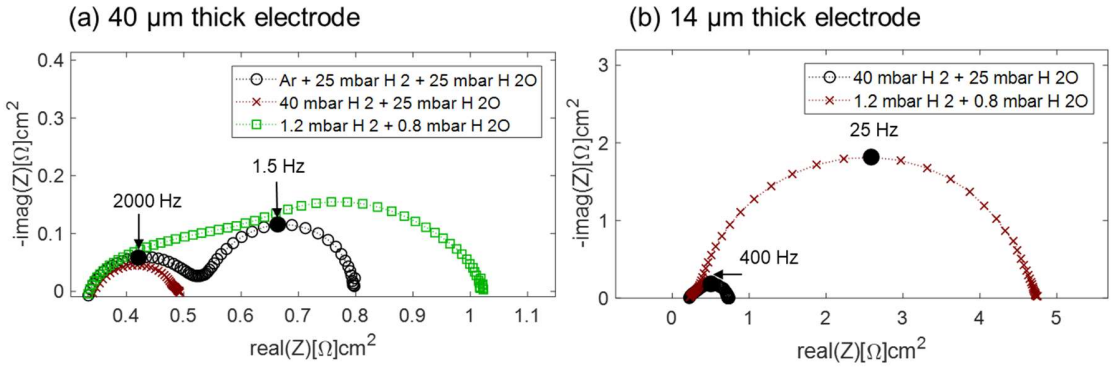

Figure 3. Impedance spectra of Ni+YSZ cermet anodes at 790°C, in different atmospheres for (a) 40 and (b) 14 µm electrode thickness.

Another characteristic of gas phase diffusion is the relatively weak temperature dependence, which causes a flattening of the Arrhenius slopes of the ASR in the high temperature region of an Arrhenius plot. For this, the ASR is simply calculated by DC resistance minus high frequency axes intercept. This is shown in Figure 4. Clearly visible, the measurements in Figure 4a exhibit a straight line with activation energies of ~0.95 eV in the Arrhenius plots, whereas the measurements in Figure 4b show a clear flattening of the slopes at higher temperature, due to the influence of gas phase diffusion, as already observed in literature (20,21).

The equivalent circuit models derived in literature are all only valid a long as gas phase diffusion does not influence the electrode impedance. Therefore meaningful equivalent circuit fitting is in the following section only considered for measurements that are plotted in in Figure 4a (40 µm thickness in 40 mbar H_2 + 30 mbar H_2O and 14 µm thickness in all conditions)

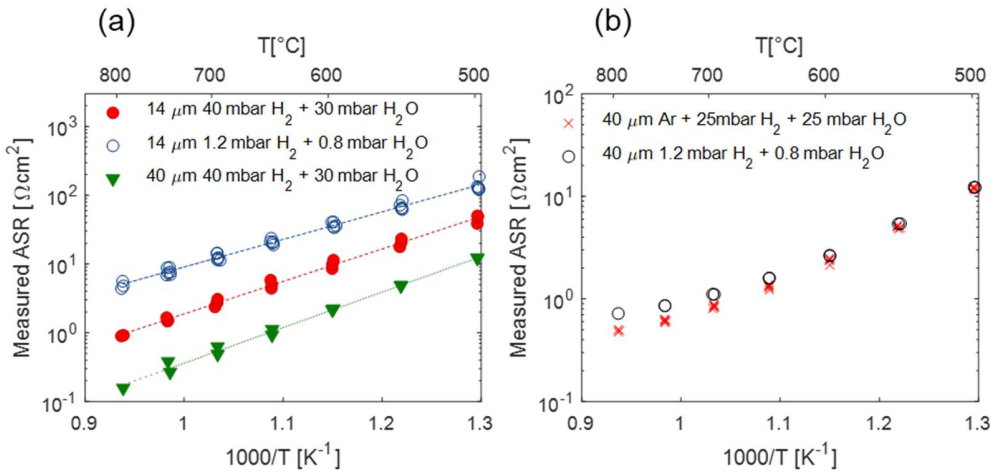

Figure 4. Measured ASR values of Ni-YSZ anodes in testing conditions, in which gas phase diffusion impedance is negligible (a), or becomes relevant at higher temperatures, causing a flattening of the Arrhenius slopes (b).

Equivalent Circuit Fitting Results

Impedance spectra were fitted after normalization to the electrode area, using the commercial software Zview. The transmission line equivalent circuit depicted in Figure 1c was used for fitting, which is a native circuit element in Zview, named *"DX11 – Bisquert 2"*, with the analytic impedance function in equation [3]. The relation of the Fitting parameter names in Zview to equation [3] is given in Table 1.

A set of impedance spectra (symbols) and fitting curves (solid lines) is plotted in Figure 5. Ni+YSZ anodes with two different thicknesses (14 and 40 µm) and different atmospheric conditions/temperatures. The circuit model has only six free parameters, and excellently describes the shape of the spectra. However, a meaningful equivalent circuit fit not only describes the shape of the spectrum, but also the numerical values of the fitting parameters must scale reasonably with varying testing conditions in order to prove the appropriateness of the circuit model.

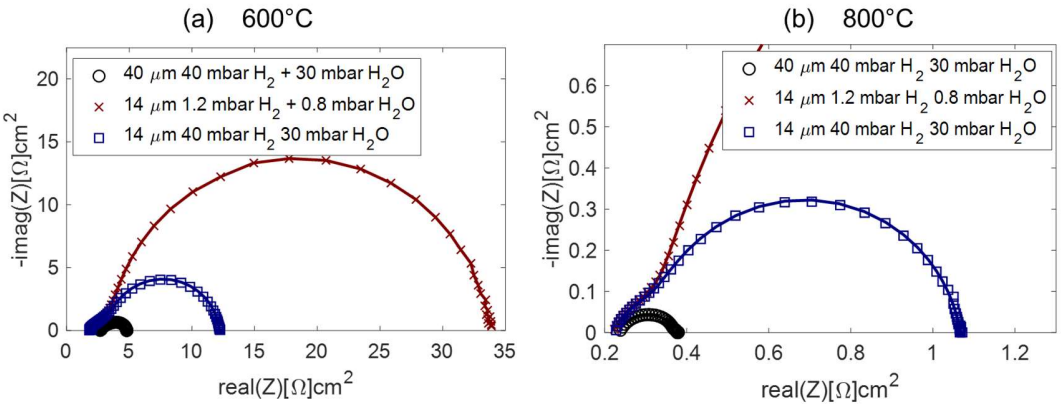

Figure 5. Impedance spectra (symbols) and equivalent circuit fits (solid lines) of Ni+YSZ electrodes with 2 different thicknesses, in different atmospheric conditions at (a) 600°C, and (b) 800°C.

Ionic conductivity and Electrochemically Active Thickness

One parameter that has a straightforward relation to the materials properties of Ni+YSZ cermet electrodes is the ion conduction resistance, which is the inverse effective ionic conductivity, and related to the specific ion conductivity of YSZ by equation [5], and the relation is depicted in Figure 6a for a 14 µm thick electrode in two different testing atmospheres. Although the shape of the spectra and total polarization resistance depends strongly on the atmosphere, the fitted effective ion conductivity is independent of the H_2 and H_2O partial pressures, as it is actually expected for YSZ. By comparing the fit result with a literature value for 8YSZ by Ahamer et al (22), we see that the slopes in the Arrhenius plot are almost identical, although the effective ion conductivity of the porous YSZ structure is 15-20 times lower than the YSZ bulk conductivity.

From equation [5] we know that this factor equals the YSZ phase tortuosity divided by YSZ volume fraction. For a typical YSZ volume fraction of 0.3, this means that the tortuosity factor is in the order of 4.5-6. This factor is actually slightly lower than what is found in literature, where this factor is typically claimed to be around 10 for screen printed Ni(O)-YSZ electrdoes (15,23,24). Unfortunately, we do not have any tomography data to claim any of these values, although we expect reasonable comparability of microstructures, since the preparation procedure is almost identical to the literature reference. Another decisive quantity is the characteristic electrochemically active thickness, which is calculated by

$$\lambda_{DC} = \lambda(\omega = 0) = \sqrt{\frac{R_{TPB}}{R_{ion}}}. \qquad [8]$$

As stated in the introduction, the impedance fit with all parameters set “free” only works as long as the electrochemically active thickness is at least half of the electrode thickness. Otherwise, the impedance function converges towards the overparametrised expression in equation [7], and one fit parameter must be constrained. Thanks to the very reliable fit of ionic conductivity for the 14 µm thick electrode, the fit for the thicker electrode could be performed by constraining the ion conductivity to the value determined from the thinner electrode, as the YSZ volume fraction and tortuosity should not depend on the thickness. With this “trick” we can now compare the electrochemically active thicknesses of the Ni-YSZ electrodes in different atmospheres, which are plotted in Figure 6b. Interestingly, the electrochemically active thickness is almost temperature independent. This means that the fit parameters R_{TPB} and R_{ion} have almost identical activation energies of 0.9-1 eV. When comparing λ_{DC} for different testing conditions, we can see that at lower H_2 and H_2O pressures, there is an increase of λ_{DC}, because of a higher TBP resistance. Also we can see that, against intuition, the thicker electrode has a significantly lower electrochemically active thickness, although testing conditions and microstructure are expected to be equal. The electrochemically active thickness λ_{DC} is also very important for SOFC manufacturers, because the optimal electrode thickness is at least 2* λ_{DC}, but not much thicker, because gas diffusion losses may increase for too thick active layers with very small pores.

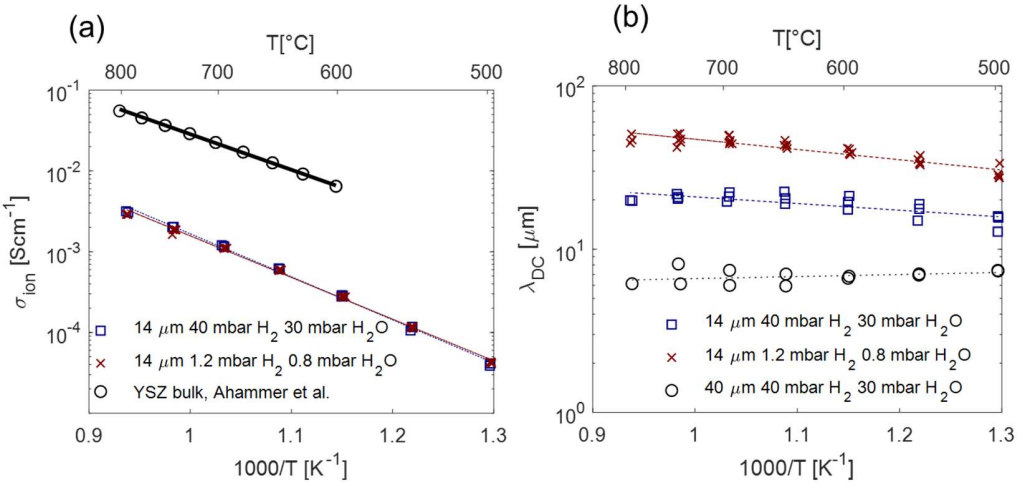

Figure 6. Fit parameters for the Ni-YSZ cells, using the equibalent circuit shown in Figure 1c. (a) effective ionic conductivity of the YSZ phase and (b) characteristic electrochemically active thickness.

Effective TPB Resistance

Another important kinetic parameter is the effective TPB resistance, which has the unconventional unit of Ωcm^3. Mechanistically, one can understand this parameter as the effective electrical resistance of the hydrogen oxidation reaction on all TPBs that are present in 1cm^3 of porous electrode. Therefore, the numerical value is small compared to the electrochemical ASR, because the electrochemically active thickness is typically in the order of 0.001 cm. In Figure 7, the effective TPB resistance values are plotted, and compared to thin film model studies (14,25).

As expected, higher H_2 and H_2O partial pressures strongly decrease the TPB resistance, and interestingly the thicker anode also has a lower TPB resistance, although testing conditions and microstructure should be rather similar. This difference cannot be explained by microstructure alone, but most likely varying amounts of impurities during cell fabrication are the result for this difference. Nevertheless, also this result is relevant, since it highlights the importance of avoiding contaminations in order to get the optimal electrode performance. To set the found values in relation to thin film model studies in literature, we assume an effective TPB density (d_{tpb} of 2µm/µm^3 = 2*10^8 cm/cm^3, as it is claimed (15,23,24) for almost equally prepared electrodes. Thin film model electrode studies in literature (25,26) estimate a resistance per unit length of TPB (LSR) at 800°C of roughly 8*10^5 Ωcm. By the relation R_{TPB} = LSR/d_{TPB}, we therefore get a value of R_{TPB} ≈ 0.004 Ωcm^3 at 800°C in 40 mbar H_2 + 30 mbar H_2O. By comparison with the impedance fitting results in Figure 7, we see that this predicted value is slightly higher than our fitting results at equal conditions. However, some uncertainty stems from the TPB length estimation. Moreover, TPB resistance values are also strongly affected by impurities, so this difference is most likely explained by the variance of the length specific resistance due to impurities.

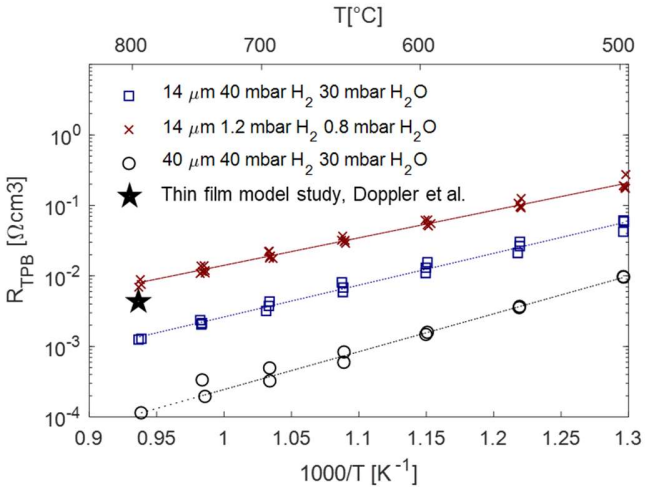

Figure 7. Effective TPB resistance of the Ni+YSZ pattern electrodes, for different testing conditions, and comparison with a model electrode reference (25).

Conclusions

We introduced a physically motivated equivalent circuit model for Ni+YSZ anodes, which is similar to the Adler-Lane-Steele model, that was originally derived for SOFC cathodes. With this model we interpret the impedance of symmetrical YSZ electrolyte supported cells with Ni+YSZ cermet electrodes. From the comparison of different gas phase compositions, temperatures and electrode thicknesses, we can draw following conclusions: Analytic impedance functions can only be used when gas phase diffusion impedance is negligible compared to the electrochemical polarisation resistance. This was achieved by using highly porous Ni foam for electrode contacting and decreasing the total pressure to 70 mbar of pure H_2+H_2O atmosphere, without any inert buffer gas.

Equivalent circuit fitting revealed values for the effective ionic conductivity of the YSZ phase and effective resistance of the TPB reaction. By comparing the effective ion conductivity to YSZ bulk, the effective cermet conductivity is about 15-20 times lower, due to tortuosity and volume fraction of the YSZ phase. The resistance of the TPB reaction in the porous electrodes depends (as expected) on the gas phase H_2 and H_2O partial pressures, whereas the effective ionic conductivity is independent of the atmospheric composition. Interestingly, the effective TPB resistance of the thicker electrode is significantly lower, which is most likely due to varying impurity amounts during electrode fabrication. When we compare the effective TPB resistance with projections gained from thin film model electrode measurements, we find that the porous electrode exhibit slightly better kinetics, which is again most likely explained by varying impurity amounts.

Overall, this work highlights how mechanistic insight into electrode processes can be gained with the aid of proper equivalent circuit modelling and impedance fitting of symmetrical electrolyte supported cells. Screen-printed Ni-YSZ electrodes are selected as one illustrative example, for which fitting results are actually in good agreement with expectations from model studies available in literature.

Acknowledgements

The financial support by the Austrian Federal Ministry of Science, Research and Economy and the National Foundation for Research, Technology and Development is gratefully acknowledged.

References

1. S. B. Adler, J. A. Lane, and B. C. H. Steele, *J. Electrochem. Soc.*, **143**, 3554–3564 (1996).
2. A. Flura et al., *J. Electrochem. Soc.*, **163**, F523–F532 (2016).
3. S. B. Adler, *Solid State Ionics*, **111**, 125–134 (1998).
4. Y. Lu, C. Kreller, and S. B. Adler, *J. Electrochem. Soc.*, **156**, B513–B525 (2009).
5. J. Bisquert, G. Garcia-Belmonte, F. Fabregat-Santiago, and A. Compte, *Electrochem Commun*, **1**, 429–435 (1999).
6. J. Bisquert, *Phys Chem Chem Phys*, **2**, 4185–4192 (2000).
7. J. Nielsen and J. Hjelm, *Electrochimica Acta*, **115**, 31–45 (2014).
8. A. Nenning, C. Bischof, A. K. Opitz, and M. Bram, *in prep*.
9. A. Opitz, M. Gerstl, and M. Bram, https://publik.tuwien.ac.at/files/publik_270713.pdf.
10. B. Hirschorn et al., *Electrochimica Acta*, **55**, 6218–6227 (2010).
11. M. C. Doppler, J. Fleig, M. Bram, and A. K. Opitz, *J. Electrochem. Soc.*, **163**, H1019–H1025 (2016).
12. M. Hendriks, J. E. Ten Elshof, H. J. M. Bouwmeester, and H. Verweij, *Solid State Ionics*, **146**, 211–217 (2002).
13. A. K. Opitz et al., *Electrochimica Acta*, **56**, 9727–9740 (2011).
14. M. C. Doppler, J. Fleig, and A. K. Opitz, *ECS Transactions*, **68**, 1383–1390 (2015).
15. J. R. Izzo et al., *J. Electrochem. Soc.*, **155**, B504–B508 (2008).
16. J. Joos, T. Carraro, A. Weber, and E. Ivers-Tiffée, *Journal of Power Sources*, **196**, 7302–7307 (2011).
17. K. Masashi, L. Marina, R.-T. Enrique, and B. Nigel, *Electrochim Acta*, **190**, 178–185 (2016).
18. B. A. Boukamp, M. Verbraeken, D. H. A. Blank, and P. Holtappels, *Solid State Ionics*, **177**, 2539–2541 (2006).
19. B. A. Boukamp and H. J. M. Bouwmeester, *Solid State Ionics*, **157**, 29–33 (2003).
20. S. Primdahl and M. Mogensen, *J. Electrochem. Soc.*, **146**, 2827–2833 (1999).
21. V. A. Rojek-Wöckner, A. K. Opitz, M. Brandner, J. Mathé, and M. Bram, *Journal of Power Sources*, **328**, 65–74 (2016).
22. C. Ahamer, A. K. Opitz, G. M. Rupp, and J. Fleig, *J. Electrochem. Soc.*, **164**, F790–F803 (2017).
23. H. Iwai et al., *Journal of Power Sources*, **195**, 955–961 (2010).
24. D. Kanno, N. Shikazono, N. Takagi, K. Matsuzaki, and N. Kasagi, *Electrochimica Acta*, **56**, 4015–4021 (2011).
25. M. Doppler, thesis, TU Wien (2018).
26. J. Mizusaki et al., *J. Electrochem. Soc.*, **141**, 2129–2134 (1994).